

Simplified method to design laterally loaded piles with optimum shape and length

Luigi Fenu^{1a}, Bruno Briseghella^{*2b} and Giuseppe Carlo Marano^{2b}

¹Department of Civil & Environment Engineering and Architecture, University of Cagliari, Via Marengo 2, 09123 Cagliari, Italy

²College of Civil Engineering, Fuzhou University, No. 2 Xue Yuan Road, University Town, Fuzhou 350108 - Fujian, China

(Received November 25, 2018, Revised March 20, 2019, Accepted March 21, 2019)

Abstract. Optimum shape and length of laterally loaded piles can be obtained with different optimization techniques. In particular, the Fully Stress Design method (FSD) is an optimality condition that allows to obtain the optimum shape of the pile, while the optimum length can be obtained through a transversality condition at the pile lower end. Using this technique, the structure is analysed by finite elements and shaped through the FSD method by contemporarily checking that the transversality condition is satisfied. In this paper it is noted that laterally loaded piles with optimum shape and length have some peculiar characteristics, depending on the type of cross-section, that allow to design them with simple calculations without using finite element analysis. Some examples illustrating the proposed simplified design method of laterally loaded piles with optimum shape and length are introduced.

Keywords: Winkler's soil; FSD method; laterally loaded piles; optimum shape and length; specific constants; simplified design

1. Introduction

Laterally loaded piles are members prevalently subjected to bending. So, even if in Geotechnics and in Foundation Structure Design they are currently called "laterally loaded piles" (Poulos and Davis 1980, Bowles 1996), they can be considered to behave as beams. Actually, in a number of engineering cases, axial loads of laterally loaded piles are negligible, as in many cases of retaining walls, harbour embankments, wind wheels and bridge abutments. Although in engineering practice they are considered as "piles in bending", in the following, when describing their mechanical behaviour and the optimization of their shape and length, we will refer to them as "beams".

In many real cases, such as in integral abutment bridges (Lan *et al.* 2017), the pile lateral displacement is to be minimized (Fenu and Serra 1995, Fenu *et al.* 2006), or on the contrary maximized (Lan *et al.* 2017), depending on the control of the pile head flexibility. Optimizing the pile shape and length (Fenu *et al.* 2018) is therefore of concern (Caner and Zia 1998, Zordan and Briseghella 2007, Briseghella and Zordan 2007-2015, Zordan *et al.* 2011, Zordan *et al.* 2011, Kim *et al.* 2013, Kim *et al.* 2014, Xu *et al.* 2017, Lavorato *et al.* 2015). Of course, while in general cylindrical piles are used (sometimes truncated-conical, or at most made of two or three cylindrical segments with different diameters (Fenu and Madama 2006),

in this research the shape of optimum piles varies with the bending moment, whose distribution along the pile depends on the applied load as well as on the soil reaction.

Nakhaee and Johari (2013) optimised the lateral load bearing capacity of piles through genetic algorithms assuming diameter, length and mechanical properties as design variables. Gandomi and Alavi (2012) implemented a neural network algorithm for designing laterally loaded piles, thus reliably predicting their performances. Imancli *et al.* (2009) defined some performance functions of laterally loaded piles in concrete driven in homogeneous clays.

Since laterally loaded piles are bended elements that behaves as beams, their optimum shape depends on the bending moment along them, as in any optimized beam (Haftka and Gürdal 1993). Moreover, since they are only laterally constrained by the surrounding soil without a point constraint at their lower end, an optimum length value can be obtained. Some authors faced the problem of how to optimise laterally loaded piles (Fenu and Serra 1995) and Fenu (2005) through variational calculus. Fenu *et al.* (2018) optimised shape and length of laterally loaded piles using a well-known optimality criterion, the Fully Stressed Design (FSD) method (Bartholomew and Morris 1976, Haftka and Gürdal 1993, Patnaik and Hopkins 1998).

The design techniques of structural optimization have been initially used in mechanical and aeronautical engineering, and have been progressively adopted also in civil engineering (Briseghella *et al.* 2013-2016, Marano *et al.* 2006, Marano *et al.* 2007, Fiore *et al.* 2016, Greco *et al.* 2016, Greco and Marano 2015, Greco *et al.* 2015, Marano *et al.* 2014, Marano and Greco 2011, Marano *et al.* 2013, Quaranta *et al.* 2014, Zordan *et al.* 2010).

Before the diffusion of evolutionary optimization

*Corresponding author, Professor

E-mail: bruno@fzu.edu.cn

^a Researcher

^b Professor

algorithms, the FSD method, herein adopted, was the optimization method more extensively used in industry (Haftka and Gürdal 1993). It is an optimality criterion leading to the minimum weight design for statically determinate structures (Haftka and Gürdal 1993), while, in most cases of statically indeterminate structures, it leads to design solutions close to the optimum.

Regarding the soil-pile interaction, in this paper the Winkler's soil model is adopted (Winkler 1867). Although many authors have proposed more sophisticated soil-pile interaction models (David and Forth 2011, Ashour and Norris 2000, Boulanger *et al.* 1999, Kim and Jeong 2011, Kavitha *et al.* 2016, McGann and Arduino 2011, Carbonari *et al.* 2012) with more complex soil constitutive laws (McGann and Arduino 2011, McGann *et al.* 2011, Chik *et al.* 2008, Ahmadi and Ahmari 2009, Juimarongrit and Ashford 2004, Broms 1964, Kok and Huat 2008, Krishnamoorthy and Sharma 2008, Phanikanth *et al.* 2010, Wakai *et al.* 1999, Yang and Jeremic 2002), for laterally loaded piles the Winkler soil model gives sufficiently reliable results (Poulos and Davis 1988, Reese and Desai 1977, Brown and Shie 1990, Han and Frost 2000).

From the results obtained by analysing laterally loaded piles by finite elements and optimising their shape and length through the FSD method coupled to a transversality condition at the pile lower end, some peculiar properties were identified. Through exploiting them, laterally loaded piles with optimum shape and length can be designed with simple mathematical operations, instead of using finite element analyses (as done in Fenu *et al.* 2018).

After a brief explanation of the analyzed problem (Section 2 and 3), the proposed simplified design method is explained in Sections 3 and 4. In Section 5, three possible applications explained with five examples are introduced. Finally, the conclusions are drawn in Section 6.

2. Model of the beam in the Winkler's medium

To optimise shape and length of a laterally loaded pile, a beam with variable cross-section $A(x)$ embedded in a Winkler's medium is considered. Length and volume of the beam are l and V , respectively. The soil reaction is proportional to the beam width, that is to the diameter $D(x)$, if circular cross-sections are adopted. This means that, by varying the cross-section along the beam, the reaction of the elastic soil varies as well, as it usually happens in engineering problems. Since the coefficient of subgrade reaction of the Winkler's medium is k_h , then the soil reaction varying along the beam is

$$k(x) = k_h D(x) \quad (1)$$

In structural optimization, it is in general convenient to express the diameter D , as well as the moment of inertia J , as proportional to, respectively, A^β and A^α , that is $D(x) = cA(x)^\beta$ and $J(x) = hA(x)^\alpha$, respectively, where c and h are dimensioned constants and α and β are real numbers (Haftka and Gürdal 1993).

The axis of the beam coincides with the abscissa axis x (Fig. 1). A horizontal force \mathbf{P}_0 laterally loads the beam at its

top end, that is assumed as the origin of the reference system (O, x, y) . Since free rotations at the beam top are allowed, for $x=0$ the moment M_0 is zero.

In general, the coefficient of subgrade reaction of a soil layer varies with its depth z . For instance, in sandy soils and in soft clays k_h linearly varies with depth (Palmer and Thompson 1948, Poulos and Davis 1980).

In overconsolidated clays k_h can be assumed as constant along the whole beam length. In fact, Davisson (1970) noted that in overconsolidated clays k_h does not vary for considerable depths, and is proportional to the undrained cohesion c_u of the clay. Therefore, the higher is the overconsolidation of the clay, the more constant is the coefficient of subgrade reaction k_h along the clay bed. A good estimation of k_h per unit pile width is $k_h = 67 c_u$ (Davisson 1970). Besides k_h , also the Young's modulus E of the beam material is assumed to be constant along the beam length.

In this problem, the differential equation of the beam in the Winkler's medium is $k(x)v(x) + M(x)'' = 0$, where $v(x)$ is the horizontal displacement, $M(x)$ is the bending moment, $M(x)''$ is its second derivative and $M(x)'$ is its first derivative, that is the shear force $S(x)$.

To identify the specific properties of optimum beams with optimum shape and length, it is convenient to use nondimensional quantities. Equations (2) define the nondimensional abscissa ξ , lateral displacement η , cross-sectional area a , diameter d , moment of inertia j , volume v , normal stress ζ , coefficient of subgrade reaction χ_h , modulus of the top force p_0 , shear s and bending moment m :

$$\begin{aligned} \xi &= \frac{x}{l} & \eta &= \frac{v}{l} & a &= A \frac{l}{V} & d &= \frac{d}{l} \\ j &= \frac{J}{Vl} & v &= \frac{V}{l^3} & \zeta &= \sigma \frac{l^{\alpha+2}}{EhV^\alpha} \\ \chi_h &= -k_h \frac{l^{\alpha+5}}{EhV^\alpha} & p_0 &= P_0 \frac{l^{\alpha+2}}{EhV^\alpha} \\ s &= S \frac{l^{\alpha+2}}{EhV^\alpha} & m &= M \frac{l^{\alpha+1}}{EhV^\alpha} \end{aligned} \quad (2)$$

From the two above mentioned relationships $D(x) = cA(x)^\beta$ and $J(x) = hA(x)^\alpha$, the nondimensional expressions of d and j as a function of a are:

$$d = \phi a^\beta \quad (3)$$

$$j = \psi a^\alpha \quad (4)$$

where both $\psi = hV^{\alpha-1}/l^{\alpha+1}$ and $\phi = cV^\beta/l^{\beta+1}$ are nondimensional, too.

2.1 Optimum shape and length of the beam

For a given type of cross-section, the nondimensional optimum shape $a(\xi)$ of a laterally loaded beam with optimum length in a Winkler's medium is a specific characteristic of all these beams, independently of geometry and material properties (Fenu *et al.* 2018). Figure 2 shows

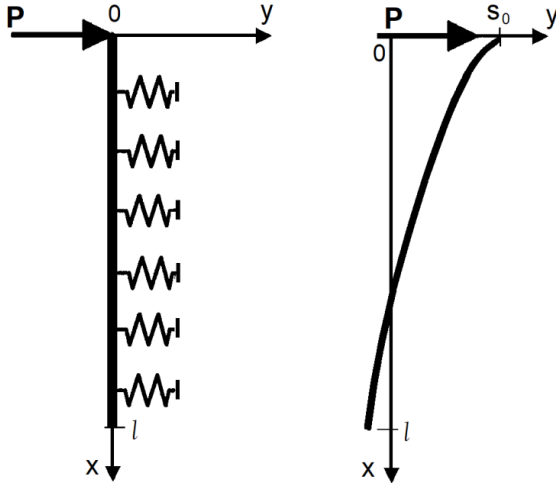


Fig. 1 Model of the beam in the Winkler's medium

the two non-dimensional cross-section distributions $a(\xi)$ of fully stressed beams with optimum length with solid and hollow circular cross-sections. These distributions were obtained through Finite Element Analysis (FEA) taking into account that, for given nondimensional values m and \bar{c} of moment M and allowable stress $\bar{\sigma}$, respectively, the FSD method allows to obtain non-dimensional diameter d and cross-sectional area a from Navier's formula as:

$$a = \left(\frac{1}{2} \frac{\phi}{\psi} \frac{1}{\nu \bar{c}} m \right)^{\frac{1}{\alpha-\beta}} \quad (5)$$

$$d = \rho \left(\frac{1}{2} \frac{\phi}{\psi} \frac{1}{\nu \bar{c}} m \right)^{\frac{\beta}{\alpha-\beta}} \quad (6)$$

where, for solid circular cross sections $\alpha=2$, $\beta=1/2$, $h=1/(4\pi)$, $c=2/\sqrt{\pi}$ and, for circular hollow sections with wall thickness t , $\alpha=3$, $\beta=1$, $h=1/(8\pi^2 t^2)$, $c=1/(\pi t)$.

Therefore, by subdividing the beam with N elements, for each i -th element with moment M_i obtained by FEA the nondimensional cross-sectional area obtained through the FSD method is:

$$a_i^{(r+1)} = \left(\frac{1}{2} \frac{\phi}{\psi} \frac{1}{\nu \bar{c}} m_i^{(r)} \right)^{\frac{1}{\alpha-\beta}} \quad (7)$$

Besides optimising the beam shape, the beam length is to be optimised as well (Fenu *et al.* 2018). For given volume V of the beam, it can be noted that among all fully stressed beams with or without optimum length, the beam with optimum length shows to have minimum top displacement v_0 . In fact, for instance, consider a fully stressed beam with solid circular cross section with given volume $V=2.219 \text{ m}^3$ and optimum length $l = 8.482 \text{ m}$, laterally loaded at the top by a force $P_0 = 500 \text{ kN}$. The mechanical characteristics of beam and Winkler's soil are $E=30 \text{ GPa}$, $\bar{\sigma}=10 \text{ MPa}$, $k_h=20 \text{ MPa}$. For same volume, both shortening and lengthening the beam with respect to the optimum causes a higher top displacement. In this example, shortening the beam from l to 6.711 m v_0 is increased from

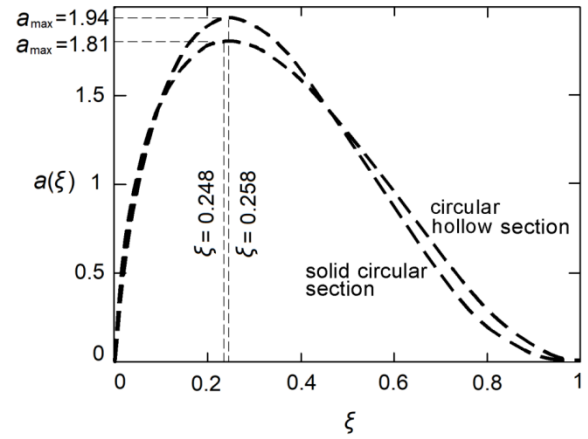


Fig. 2 Distribution of the nondimensional cross-section along the beam for circular solid and hollow sections

26.4 mm to 26.7 mm, that is by only 1%, while lengthening the beam from l to 13 m v_0 is increased from 26.4 mm to 27.8 mm, that is by 5.3%. Too long beams result longer than necessary, and the excess of material leads to a change of the sign of the moment M , thus causing the insertion of an inner hinge with $A=0$ for $M=0$. To minimize v_0 through varying the beam length, a transversality condition at the beam lower end is necessary. Considering the nondimensional displacement η_0 of the beam top end, namely:

$$\eta_0 = \int_0^1 \frac{1}{p_0} \left(\frac{m^2}{a^\alpha} - \frac{m^{\pi^2}}{\chi_h \phi a^\beta} \right) d\xi \quad (8)$$

the condition that, for given volume, the integral of $a(\xi)$ along the beam is equal to $v=1$ leads to define the auxiliary functional:

$$\eta_0^* = \int_0^1 \frac{1}{p_0} \left[\left(\frac{m^2}{a^\alpha} - \frac{m^{\pi^2}}{\chi_h \phi a^\beta} \right) + \Lambda_1 a \right] d\xi \quad (9)$$

To minimize η_0^* through varying the length of the optimum shape beam, consider the integrand function F of the functional η_0^* in order to define the transversality condition at the beam lower end, that is:

$$[F - (\phi^l - m^l) dF_{m^l} / dx]_{\xi=\xi_l=1} = 0 \quad (10)$$

where $\xi_l = x_l / l$ and $x_l = l$.

Since $\phi^l=0$ because the abscissa axis is of course not inclined to itself, then, for $\xi=\xi_l=1$, equation (10) leads to:

$$[m^l]_{\xi=\xi_l=1} = 0 \quad (11)$$

This transversality condition shows that if the beam length is optimum, it is then necessary to have a flex point ($m^l=0$) at the beam lower end ($x_l=l$), where also the boundary conditions $m^l=m=0$ must be satisfied.

The optimization procedure is summarized in Figure 3. In the following it will be shown that the optimum length does not depend on the magnitude of the applied force P_0 . Of course, since l is independent of P_0 for given beam volume and given stiffness of the material of soil and beam

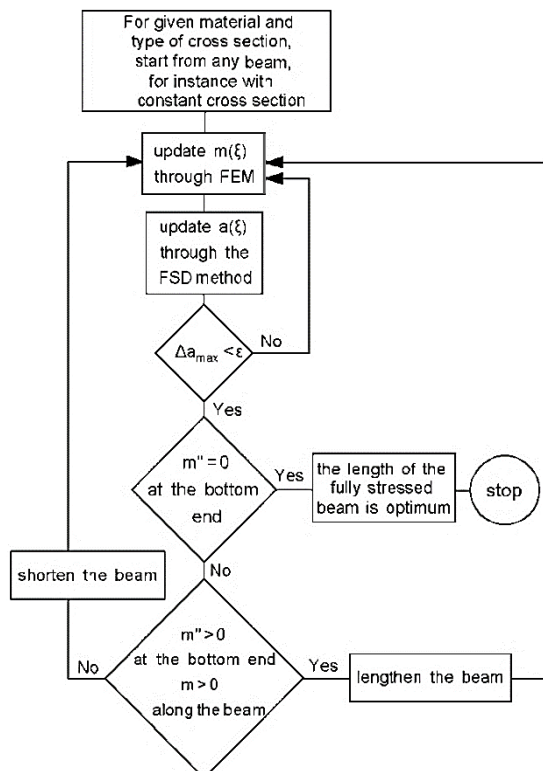


Fig. 3 Numerical algorithm to design any fully stressed beams with optimum length in a Winkler's medium

(i.e. k_h and E respectively), the higher is P_0 , the higher is the required allowable stress $\bar{\sigma}$.

3. Peculiar characteristics of laterally loaded beams with optimum shape and length

Besides having the same nondimensional cross-sectional area distribution $a(\xi)$, laterally loaded beams with optimum shape and length with given type of cross-section are characterized by some specific constants, determined as follows.

First, for given type of cross section, the product between χ_h and the average diameter d_m has shown to be always constant. Since for ξ varying in the interval $[0,1]$, the integral of $d(\xi)$ coincides with the average value d_m of d , then:

$$C = \chi_h \int_0^1 d(\xi) d\xi = \text{const} \quad (12)$$

This means that C results independent from the mechanical properties of the beam and soil materials, as well as of any constant characteristic of the cross section, i.e. the wall thickness of hollow sections.

Numerical computations show that, for solid circular cross sections and circular thin-walled hollow sections, C is equal to, respectively, 329 and 101.

Also, say B the integral of $a(\xi)^\beta$, that is:

$$B = \int_0^1 a(\xi)^\beta d\xi \quad (13)$$

Therefore, since $a(\xi)$ is assigned for given type of cross-section and β is a constant, then B is a constant as well.

Numerical computations show that for solid circular cross-sections B is 0.9, while, from (15), for circular thin-walled hollow sections B is 1, as, for $\beta=1$, the integral of $a(\xi)^\beta$ is 1.

Also, since $d(\xi) = \phi a(\xi)^\beta$, by integrating both sides of this equation and taking into account that ϕ is independent of ξ , we obtain:

$$d_m = \int_0^1 d(\xi) d\xi = \phi \int_0^1 a(\xi)^\beta d\xi = \phi B \quad (14)$$

The following constant D can be also defined:

$$D = \chi_h \phi \quad (15)$$

as, for (12), $C = \chi_h \phi B$ is a constant and, for (13), B is a constant as well, meaning that also the product $\chi_h \phi$, and therefore D , must be a constant. For solid circular cross-sections and circular thin-walled hollow sections, D is equal to, respectively, 365.5 and 101.

Finally, from (5) one obtains:

$$a(\xi) = g^{1/(\alpha-\beta)} m(\xi)^{1/(\alpha-\beta)} \quad (16)$$

where

$$g = \frac{\phi}{2 \nu \nu \bar{c}} \quad (17)$$

Function $f(\xi) = a(\xi)^{(\alpha-\beta)} = g m(\xi)$ can be therefore defined. Since α and β are constant, then $f(\xi)$, like $a(\xi)$, is another peculiar characteristic of laterally loaded beams with optimum shape and length for each type of cross-section. A further constant parameter $Q = df/d\xi|_{\xi=0}$, is hence defined, with $Q = g dm/d\xi|_{\xi=0}$. It is worth noting that the boundary condition of the derivative of m at the beam top is $\bar{p}_0 = dm/d\xi|_{\xi=0}$, where

$$\bar{p}_0 = \bar{P}_0 \frac{l^{\alpha+2}}{EhV^\alpha} \quad (18)$$

is the nondimensional lateral force applied at the beam top for which the stress σ coincides with the allowable stress $\bar{\sigma}$ in each beam section, as required by the FSD method. This means that \bar{p}_0 is the nondimensional lateral load bearing capacity of the beam. After calculating numerically $\bar{p}_0 = dm/d\xi|_{\xi=0}$, the constant Q is then easily evaluated as

$$Q = \bar{p}_0 g \quad (19)$$

Knowing Q and calculated g from (17), the lateral load bearing capacity \bar{P}_0 of the beam is easily calculated through combining (19) with (18). It means that if P_0 is higher than \bar{P}_0 , then the stress σ in the beam exceeds the allowable stress $\bar{\sigma}$.

The values of the constants B , C , D and Q characterizing fully stressed beams with optimum length with circular solid and circular hollow sections are listed in Table 1.

Table 1 Constants characterizing fully stressed beams with optimum length for given type of cross section

| | B | C | D | Q |
|-----------------|-----|-----|-------|------|
| Circular solid | 0.9 | 329 | 365.5 | 22.5 |
| Circular hollow | 1 | 101 | 101 | 25.5 |

4. Simplified design of laterally loaded piles with optimum shape and length using the constants B, C, D, Q

To design laterally loaded beams with optimum shape and length through the FSD method, structural analysis by finite elements is usually necessary, as discussed in section 2.1.

The four constants defined in the previous section allow to design optimum beams without using FEA with only simple mathematical operations, namely algebraic sums, products, divisions and exponentiations.

In fact, equation (12) can be expressed as $C = \chi_h d_m$, that is, for (14), $C = \chi_h \phi B$. By explicitly expressing the nondimensional ratios χ_h and ϕ , one obtains:

$$C = \frac{B c k_h l^{\alpha-\beta+4}}{E h V^{\alpha-\beta}} \quad (20)$$

Given the beam volume V , from equation (20) the optimum length l is obtained as:

$$l = \left(\frac{C E h V^{\alpha-\beta}}{c B k_h} \right)^{\frac{1}{\alpha-\beta+4}} \quad (21)$$

It can be noted that l only depends on the given volume V , on the mechanical properties of soil and beam through E and k_h , and on the type of cross-section through the constant $C, B, h, c, \alpha, \beta$, as well as through the nondimensional mass distribution $a(\xi)$ related to this type of cross-section.

From (16), the nondimensional moment is also obtained:

$$m(\xi) = \mathcal{G} a(\xi)^{\alpha-\beta} \quad (22)$$

It depends on the nondimensional mass distribution $a(\xi)$ raised to the difference between α and β (both depending on the type of cross-section), and multiplied by the factor $\mathcal{G} = \phi(2\psi\bar{c})$. For (17), \mathcal{G} depends on the optimum beam length l (through ϕ and ψ), on its volume (through ϕ, ψ and v), on the allowable stress through \bar{c} , as well as on the type of cross-section through c, h, α and β , that are all present in the expressions of ϕ, ψ and \bar{c} .

Therefore, after obtaining l for given volume, material properties and type of cross-section, \mathcal{G} is obtained from (17). From (19), \bar{p}_0 is then obtained as

$$\bar{p}_0 = \frac{Q}{\mathcal{G}} \quad (23)$$

thus obtaining the lateral load bearing capacity \bar{P}_0 through combining (23) with (18). Since the beam is fully stressed, then \bar{P}_0 must be equal to the applied lateral load P_0 , in order to have $\sigma = \bar{\sigma}$ in all the beam sections. Higher values of P_0 would cause higher stress level in the beam, with $\sigma > \bar{\sigma}$.

Conversely, the magnitude of the applied force \mathbf{P}_0 can be assigned. For given beam volume V , the optimum length l is still obtained from (21). Calculated the nondimensional applied force p_0 , elimination of \mathcal{G} between (17) and (19) allows to calculate \bar{c} . The allowable material stress $\bar{\sigma}$ of the beam to be used in order to resist the force \mathbf{P}_0 is hence obtained. Also, calculated \mathcal{G} from (17) or, conversely, from (19), the moment along the beam is also obtained through (22).

Finally, a different design case can also occur, in which both the applied force \mathbf{P}_0 and the allowable stress $\bar{\sigma}$ are assigned. In this case, besides the optimum length l , also the beam volume V is unknown. Moreover, the optimum length cannot be obtained from (21), because, however, for given soil, beam material and type of cross-section, this equation shows that l depends on V .

This design problem can be easily solved by trial-and-error through comparison of the nondimensional applied force $p_0 = P_0 l^{(\alpha+2)} / (E h V^\alpha)$ with the nondimensional resistance force \bar{p}_0 calculated through (18).

For this aim, a tentative value of V must be assigned. Hence, at a 1-st step, a 1-st value of l can be calculated through (21), as well as a 1-st value of the nondimensional applied force $p_{0,A} = P_0 l^{\alpha+2} / (E h V^\alpha)$ and a 1-st value of \mathcal{G} calculated through (17), thus allowing to compare the 1-st value of p_0 with the 1-st value of the nondimensional resistance force \bar{p}_0 obtained from (22). If V is too high, p_0 is higher than \bar{p}_0 , and V must be decreased. Conversely, if V is too low, p_0 is lower than \bar{p}_0 , and V must be increased. When same values of p_0 and \bar{p}_0 are achieved, the actual beam volume and, through (21), the optimum length required to minimize the top displacement of the fully stressed laterally loaded beam are obtained.

In all the cases considered, after obtaining the actual values of l, V and \mathcal{G} , the actual moment distribution $M(x) = m(\xi) E h V^\alpha / l^{\alpha+1}$ in each beam section is obtained through evaluating the nondimensional moment distribution $m(\xi)$ from (22).

5. Examples

The above mentioned design method allows a quick optimum design of laterally loaded piles in a Winkler's medium with only few mathematical operations and only one exponentiation, provided that the nondimensional mass distribution is known in advance. This means that once a finite element analysis has been performed for a specific design case, the corresponding nondimensional mass distribution can be employed in any design case where the same type of cross-section is adopted.

In this paper the two cases of solid and hollow circular sections are considered. When reference is made to laterally loaded piles, hollow sections and open sections are used with special concretes as textile reinforced concrete and ultra-high-performance concrete, while circular solid sections are usually adopted when normal concrete is used.

Ng *et al.* (2015) investigated the use of ultra-high performance concrete (UHPC) in piles of integral abutment bridges, using different sections to resist lateral loads, i.e. T sections as well as quadrangular, octagonal and circular hollow sections (Fig. 4).

Wall thickness 5 cm was adopted. With similar technique, ultra-high performance concrete has been also used to manufacture the lower segments of big wind-turbine towers height 135 m, as those of one of the largest wind farm in the world in Estinnes, Belgium. Circular hollow section piles can be also manufactured using centrifuged concrete reinforced with steel bars or steel meshes. In both

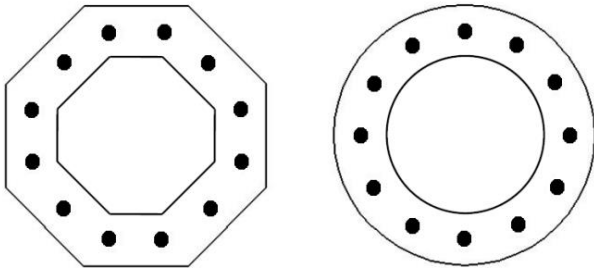


Fig. 4 Hollow sections of laterally loaded UHPC piles for integral abutment bridges

cases, the material properties are much better than those of normal concrete, as shown in the examples 1-4 of this section. In the following, the example of easy design of laterally loaded piles with hollow section using high performance concrete is reported. The simplified design procedure herein proposed allows to easily design all laterally loaded piles in UHPC with different open and hollow sections, provided that for any pile with a specific cross-section, its nondimensional optimised mass distribution (that is specific of this cross-section for all the optimised laterally loaded piles with any load and material properties) is available.

Normal concrete is instead more appropriate for circular solid section piles with optimum shape and length, that can be constructed by first prefabricating a hollow section pile with same shape made of centrifuged concrete, and, after embedding it into the soil, by then pouring the fluid concrete into the hollow-section pile (Fenu *et al.* 2018). A similar procedure is used in “Multiton” piles (Fenu 2006), that are manufactured with steel tubes with different diameters (the deeper the smaller) and, after embedding, are then filled in-situ with concrete to improve their load bearing capacity,

Besides in Geotechnics, laterally loaded beams in a Winkler’s medium are used also in other fields of civil and mechanical engineering. Consider for instance the case of a steel dowel fastener embedded in wood and subjected to a shear force at its head, i.e. in concrete-timber composite beams or in steel-to-timber shear joints (Fig. 5). A steel dowel fastener with optimum shape and length can be designed as a steel beam in a Winkler’s medium laterally loaded at its head by the joint shear force.

In the following, five examples showing the applicability of the proposed method to different cases are introduced.

Example 1. Design a fully stressed pile in concrete with optimum shape and length with solid circular cross-section. This type of cross-section is characterized by $\alpha=2$, $\beta=1/2$, $h=1/(4\pi)$ and $c=2/\sqrt{\pi}$ (see Section 3).

Elastic modulus and allowable stress of the beam material are $E=30$ GPa and $\bar{\sigma}=10$ MPa, respectively; the coefficient of subgrade reaction of the soil is $k_h=20$ MPa/mm, corresponding, for $k_h=67c_u$, to a clayly soil with $c_u=0.3$ MPa.

The pile volume is assigned to be $V=2.219$ m³, a volume value that is of the same magnitude order of the volume of an optimised cylindrical laterally loaded pile with same type

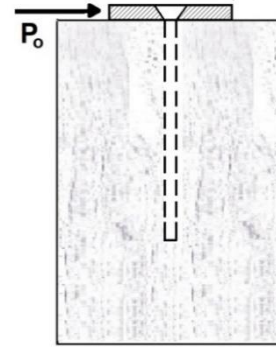


Fig. 5 Steel-to-timber shear joint connecting a steel sheet and a wood member through a steel dowel fastener embedded in wood

of cross-section. The lateral load is $P_0=500$ kN.

Since a solid circular cross-section is used, the specific constants to be used for carrying out a simplified design of the pile with optimum shape and length are the ones of the first row in Table 1.

The design data are therefore: $V=2.219$ m³, $P_0=500$ kN, $E=30$ GPa, $\bar{\sigma}=10$ MPa, $k_h=20$ MPa/mm.

From the simple operations described in the previous section, one obtains:

$$\begin{aligned} l &= 8.482 \text{ m} & p_0 &= 0.22 \\ \phi &= 6.805 \times 10^{-2} & \psi &= 2.894 \times 10^{-4} \\ \nu &= 3.637 \times 10^{-3} & \bar{c} &= 3.167 \times 10^3 \\ g &= 102.1 & \bar{p}_0 &= 0.22 \end{aligned} \quad (24)$$

The nondimensional applied load p_0 results equal to the nondimensional resistant force $\bar{p}_0 = Q/g$. This means that the stress in any section is equal to the allowable stress $\bar{\sigma}$. Checking this in the pile section with maximum bending moment where $a_{\max}=1.94$, one obtains:

$$\begin{aligned} m_{\max} &= 0.026 & M_{\max} &= 510.0 \text{ kNm} & j_{\max} &= 1.09 \cdot 10^{-3} \\ J_{\max} &= 0.0680 \text{ m}^4 & A_{\max} &= 0.5076 \text{ m}^2 & D_{\max} &= 0.934 \text{ m} \end{aligned} \quad (25)$$

and, from Navier formula, $\sigma=10$ MPa, that is $\sigma=\bar{\sigma}$. The same procedure can be repeated for any section of the pile, still obtaining $\sigma=\bar{\sigma}$, as the laterally loaded pile is fully stressed in any section, in accordance with what required by the FSD method.

It is worth noting that, assigning the same pile volume, if $P_0 > 500$ kN, then $p_0 = P_0 l^{-2} / (E h V) = Q/g = 0.22$. The pile shape and length would be the same, but $P_0 > 500$ kN would lead to $\sigma > \bar{\sigma}$.

Example 2. Consider a pile with circular solid section and same material properties than that of the previous example, with given lateral load $P_0=700$ kN, but with unknown pile volume.

To find volume and optimum length of the laterally loaded pile, a trial-and-error procedure is carried out.

At the 1-st step, $V^{(1)}=3$ m³ is tried, chosen to be of the same magnitude order of the volume of an optimised cylindrical laterally loaded pile with same type of cross-section.

For each step, a procedure similar to that of the previous example is followed. After the 1-st step the results are:

$$\begin{aligned}
l^{(1)} &= 9.209 \text{ m} & p_0^{(1)} &= 0.234 \\
\phi^{(1)} &= 6.994 \times 10^{-2} & \psi^{(1)} &= 3.057 \times 10^{-4} \\
\nu^{(1)} &= 3.842 \times 10^{-3} & \bar{c}^{(1)} &= 283.795 \\
\mathcal{G}^{(1)} &= 104.91 & \bar{p}_0^{(1)} &= 0.214
\end{aligned} \quad (26)$$

Since $p_0^{(1)} > \bar{p}_0^{(1)}$, then the pile volume is to be increased. Trying $V^{(2)} = 3.7 \text{ m}^3$, one obtains:

$$\begin{aligned}
l^{(2)} &= 9.751 \text{ m} & p_0^{(2)} &= 0.194 \\
\phi^{(2)} &= 7.129 \times 10^{-2} & \psi^{(2)} &= 3.176 \times 10^{-4} \\
\nu^{(2)} &= 3.991 \times 10^{-3} & \bar{c}^{(2)} &= 262.957 \\
\mathcal{G}^{(2)} &= 106.929 & \bar{p}_0^{(2)} &= 0.210
\end{aligned} \quad (27)$$

Contrary to the 1-st step, at this 2-nd step $p_0^{(2)} < \bar{p}_0^{(2)}$, hence the pile volume is to be decreased.

Trying $V^{(3)} = (V^{(1)} + V^{(2)})/2 = 3.35 \text{ m}^3$, one obtains:

$$\begin{aligned}
l^{(3)} &= 9.490 \text{ m} & p_0^{(3)} &= 0.212 \\
\phi^{(3)} &= 7.065 \times 10^{-2} & \psi^{(3)} &= 3.119 \times 10^{-4} \\
\nu^{(3)} &= 3.920 \times 10^{-3} & \bar{c}^{(3)} &= 272.632 \\
\mathcal{G}^{(3)} &= 105.968 & \bar{p}_0^{(3)} &= 0.212
\end{aligned} \quad (28)$$

Since $p_0^{(3)} = \bar{p}_0^{(3)}$, at the 3-rd step convergence is achieved.

Checking the stress at the section with maximum bending moment, that is the section with maximum cross-sectional area $a_{\max} = 1.94$, one obtains:

$$m_{\max} = 0.025 \quad M_{\max} = 799.4 \text{ kNm} \quad j_{\max} = 1.17 \cdot 10^{-3} \quad (29)$$

$$J_{\max} = 0.0373 \text{ m}^4 \quad A_{\max} = 0.68486 \text{ m}^2 \quad D_{\max} = 0.934 \text{ m}$$

and, from Navier formula, $\sigma = 10 \text{ MPa}$, that is $\sigma = \bar{\sigma}$, in accordance with what required by the FSD method. Checking any other section, one would still obtain $\sigma = \bar{\sigma}$.

The shape of this laterally loaded pile is similar to that of the hollow section one in Figure 5, because circular solid and circular hollow sections have similar distribution of the nondimensional cross-sectional area (see Fig. 2). Of course pile volume and length are very different, because hollow sections are more efficient than solid sections.

Example 3. A fully stressed beam with optimum shape and length with hollow circular cross-section with wall thickness $t = 50 \text{ mm}$ is to be designed. This type of cross-section is characterized by $\alpha = 3$, $\beta = 1$, $h = 1/(8\pi^2 t^2)$, $c = 1/(\pi t)$ (see Section 3)

The coefficient of subgrade reaction of the soil is $k_h = 5 \text{ MPa/mm}$. Since to prefabricate a hollow-section pile ultra-high performance concrete or centrifuged concrete reinforced by steel meshes can be used, concrete with higher mechanical properties is considered, for instance with $E = 45 \text{ GPa}$ and $\bar{\sigma} = 80 \text{ MPa}$.

Since a circular hollow section is used, the specific constants to be used for carrying out the simplified design of this pile with optimum shape and length are the ones of the second row in Table 1.

For given lateral load $P_0 = 820 \text{ kN}$, following the same procedure as in the previous Example 1, the pile volume is assigned to be $V = 0.215 \text{ m}^3$, thus obtaining:

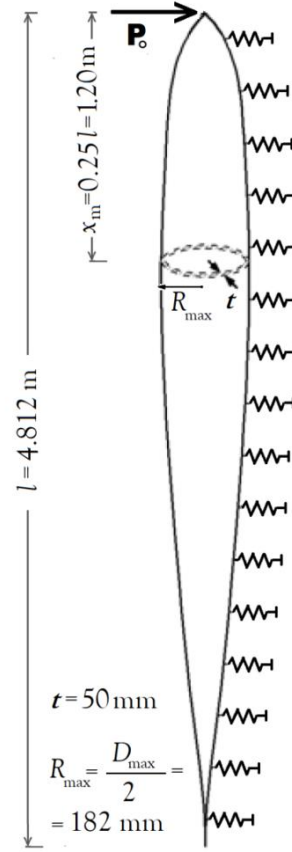


Fig. 6 Hollow section pile with optimum shape and length of Example 4

$$\begin{aligned}
l &= 5.675 \text{ m} & p_0 &= 2.135 \\
\phi &= 4.250 \times 10^{-2} & \psi &= 2.255 \times 10^{-4} \\
\nu &= 1.176 \times 10^{-3} & \bar{c} &= 6.705 \times 10^3 \\
\mathcal{G} &= 11.945 & \bar{p}_0 &= 2.135
\end{aligned} \quad (30)$$

Therefore p_0 results equal to the nondimensional resistant force $\bar{p}_0 = Q/\mathcal{G}$, and the stress σ must be equal to the allowable stress $\bar{\sigma}$. Calculating σ in the section with maximum moment and $a_{\max} = 1.81$, similarly to the previous examples one obtains:

$$\begin{aligned}
m_{\max} &= 0.274 & M_{\max} &= 597.8 \text{ kNm} & j_{\max} &= 1.34 \times 10^{-3} \\
J_{\max} &= 1.62 \times 10^{-3} \text{ m}^4 & A_{\max} &= 0.0685 \text{ m}^2 & D_{\max} &= 0.486 \text{ m}
\end{aligned} \quad (31)$$

Checking then the maximum moment section we obtain $\sigma = M_{\max} 0.5 D_{\max} / J_{\max} = 89.17 \text{ MPa}$, showing that σ practically coincides with $\bar{\sigma}$, in accordance with what required by the FSD method. The same procedure can be repeated for any beam section, still obtaining that the beam is fully stressed in any section. It is worth noting that while for solid cross sections the method is exact, for hollow sections σ is found to slightly differ from $\bar{\sigma}$, namely the ratio σ over $\bar{\sigma}$ is 0.991 instead of 1. This difference is due to the fact that the walls of a hollow section with given wall thickness tends to

merge close to the pile ends. Nevertheless, the error is negligible by an engineering point of view.

If $P_0 > 820 \text{ kN}$, then $p_0 = P_0 l^{\alpha+2} / (EhV^\alpha) > \bar{p}_0 = 2.135$, and σ becomes higher than $\bar{\sigma}$. The higher is P_0 the greater is σ with respect to $\bar{\sigma}$.

Example 4. Consider a pile with circular hollow section and same material properties than that of the previous example, but with given lateral force $P_0 = 500 \text{ kN}$, and unknown beam length and volume.

Similarly to the Example 2, to find both volume and optimum length of the beam, a trial-and-error procedure is performed, starting with $V^{(1)} = 0.15 \text{ m}^3$ at the 1-st step. One then obtains:

$$\begin{aligned} l^{(1)} &= 5.034 \text{ m} & p_0^{(1)} &= 2.101 \\ \phi^{(1)} &= 3.768 \times 10^{-2} & \psi^{(1)} &= 1.775 \times 10^{-4} \\ \nu^{(1)} &= 1.176 \times 10^{-3} & \bar{c}^{(1)} &= 8.519 \times 10^3 \\ \mathcal{G}^{(1)} &= 10.598 & \bar{p}_0^{(1)} &= 2.406 \end{aligned} \quad (32)$$

Since $p_0^{(1)} < \bar{p}_0^{(1)}$, then at the 2-nd step the pile volume is to be decreased.

Trying $V^{(2)} = 0.11 \text{ m}^3$, one obtains:

$$\begin{aligned} l^{(2)} &= 4.540 \text{ m} & p_0^{(2)} &= 3.177 \\ \phi^{(2)} &= 3.398 \times 10^{-2} & \psi^{(2)} &= 1.443 \times 10^{-4} \\ \nu^{(2)} &= 1.176 \times 10^{-3} & \bar{c}^{(2)} &= 1.048 \times 10^4 \\ \mathcal{G}^{(2)} &= 9.557 & \bar{p}_0^{(2)} &= 2.668 \end{aligned} \quad (33)$$

Contrary to the 1-st step, at this 2-nd step $p_0^{(2)} > \bar{p}_0^{(2)}$, hence the beam volume is to be increased.

Trying $V^{(3)} = (V^{(1)} + V^{(2)})/2 = 0.13 \text{ m}^3$, one obtains:

$$\begin{aligned} l^{(3)} &= 4.80 \text{ m} & p_0^{(3)} &= 2.534 \\ \phi^{(3)} &= 3.593 \times 10^{-2} & \psi^{(3)} &= 1.613 \times 10^{-4} \\ \nu^{(3)} &= 1.176 \times 10^{-3} & \bar{c}^{(3)} &= 9.372 \times 10^3 \\ \mathcal{G}^{(3)} &= 10.104 & \bar{p}_0^{(3)} &= 2.524 \end{aligned} \quad (34)$$

Since $p_0^{(3)}$ is only slightly higher than $\bar{p}_0^{(3)}$, then the volume is only slightly increased to $V^{(4)} = 0.131 \text{ m}^3$, thus obtaining:

$$\begin{aligned} l^{(4)} &= 4.812 \text{ m} & p_0^{(4)} &= 2.517 \\ \phi^{(4)} &= 3.602 \times 10^{-2} & \psi^{(4)} &= 1.622 \times 10^{-4} \\ \nu^{(4)} &= 1.176 \times 10^{-3} & \bar{c}^{(4)} &= 9.324 \times 10^3 \\ \mathcal{G}^{(4)} &= 10.130 & \bar{p}_0^{(4)} &= 2.517 \end{aligned} \quad (35)$$

Since $p_0^{(4)} = \bar{p}_0^{(4)}$, at the 4-th step convergence is finally achieved. Figure 6 shows the optimum shape and length of this laterally loaded pile.

Similarly to the previous example, the stress at the section with maximum bending moment and $a_{\max} = 1.81$ is checked. To this aim, one first calculates:

$$m_{\max} = 0.323 \quad M_{\max} = 309.1 \text{ kNm} \quad j_{\max} = 9.62 \times 10^{-4} \quad (36)$$

$$J_{\max} = 6.06 \times 10^{-4} \text{ m}^4 \quad A_{\max} = 0.0493 \text{ m}^2 \quad D_{\max} = 0.364 \text{ m}$$

From Navier formula, one obtains $\sigma = 92.7 \text{ MPa}$, that is $\sigma \approx \bar{\sigma}$, in accordance with the FSD method. As in the previous example, the small difference between σ and $\bar{\sigma}$ is due to the wall merging in the sections close to the beam ends. Figure 7 shows the actual moment distribution along the hollow section pile.

Example 5. Consider a steel dowel fastener embedded in

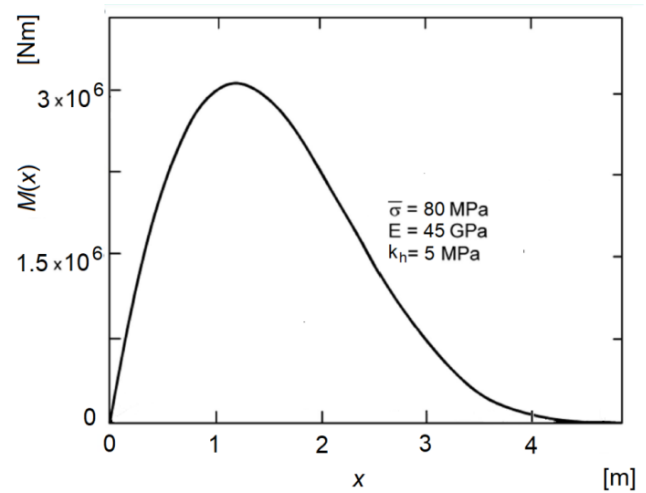


Fig. 7 Moment $M(x)$ along the hollow section pile of Figure 6

wood and subjected to a shear force $P_0 = 2.9 \text{ kN}$ at the head (See Fig.5). Fastener length and volume to be optimised are unknown. From wood stiffness and steel material properties, it is assumed that $k_h = 10500 \text{ MPa}$, $E = 210 \text{ GPa}$, and $\bar{\sigma} = 300 \text{ MPa}$.

Similarly to the previous Examples 2 and 4, to solve this design problem, a trial-and-error design procedure is necessary. After few steps, at the final n-th step, for $V^{(n)} = 5000 \text{ mm}^3$ one obtains

$$\begin{aligned} l^{(3)} &= 112 \text{ mm} & p_0^{(3)} &= 1.076 \\ \phi^{(3)} &= 6.774 \times 10^{-2} & \psi^{(3)} &= 2.868 \times 10^{-4} \\ \nu^{(3)} &= 3.604 \times 10^{-3} & \bar{c}^{(3)} &= 1.382 \times 10^3 \\ \mathcal{G}^{(3)} &= 23.71 & \bar{p}_0^{(3)} &= 1.076 \end{aligned} \quad (37)$$

with convergence achieved, as $p_0^{(n)} = \bar{p}_0^{(n)}$.

The stress at the section with maximum bending moment and maximum nondimensional cross-sectional area $a_{\max} = 1.94$ is finally checked.

After calculating:

$$m_{\max} = 0.114 \quad M_{\max} = 34 \text{ Nmm} \quad j_{\max} = 1.08 \times 10^{-3} \quad (38)$$

$$J_{\max} = 602 \times 10^{-4} \text{ mm}^4 \quad A_{\max} = 86.97 \text{ mm}^2 \quad D_{\max} = 0.364 \text{ m}$$

from Navier formula, one obtains $\sigma = 300 \text{ MPa}$, that is $\sigma = \bar{\sigma}$, as required by the FSD method.

It is worth noting that in the mass production of steel dowel fasteners, even a low mass saving can result in a high production cost saving.

6. Conclusions

A method to easily design laterally loaded beams with optimum shape and length embedded in a Winkler's medium has been illustrated. The proposed simplified design method has been developed through identifying some nondimensional constants that are specific of all

optimum laterally loaded beams in a Winkler's medium with same cross-section type, and that are independent of applied load, beam length and volume, and material properties. A further peculiar property is that all the optimum laterally loaded beams with same type of cross-section have same nondimensional mass distribution. To allow the application of the method in some design problems frequently faced in structural engineering, the mass distribution related to any embedded beam with circular solid and hollow cross-section (both available from a previous research and calculated by finite elements) has been provided.

Among the laterally loaded beams embedded in a Winkler's medium, in civil engineering laterally loaded piles are the most commonly used, for instance in the foundations of wind turbines, integral abutment bridges, retaining walls, harbour embankments and in structures subjected to seismic loads. The examples developed in the paper show how the simplified design of laterally loaded piles with optimum shape and length, otherwise performed by finite elements, can be easily carried out with simple mathematical operations. Starting from conventional cylindrical piles, the developed method leads to innovative optimal shapes, that nowadays can be obtained using ultra-high performance concrete and cement composites as textile reinforced concrete and ferrocement. Other interesting applications can be proposed both in the field of structural engineering and in mechanical engineering. For instance, the effectiveness of the design method has been also shown through an application to steel dowel fasteners embedded in a wood element and subjected to a shear force at the fastener head. It's an interesting optimization problem that could lead to a significant material saving in the mass production of steel dowel fasteners.

Acknowledgments

The research was supported by the Recruitment Program of Global Experts Foundation (Grant No. TM2012-27) and National Natural Science Foundation of China (Grant No. 51778148) and by the FIR fund of the University of Cagliari (Cagliari, Italy). The authors would also like to acknowledge the Sustainable and Innovative Bridge Engineering Research Center (SIBERC) of the College of Civil Engineering of the Fuzhou University (Fuzhou, China), and the Department of Civil Engineering, Environmental Engineering and Architecture of the University of Cagliari (Cagliari, Italy).

References

- Ahmadi, M.M. and Ahmari, S. (2009), "Finite element modelling of laterally loaded piles in clay", *Proceedings of the Institution of Civil Engineering - Geotechnical Engineering*, **162**(3), 151-163. <https://doi.org/10.1680/geng.2009.162.3.151>.
- Ashour, M. and Norris, G. (2000), "Modelling lateral soil-pile response based on soil-pile interaction", *J. Geotech. Geoenviron. Eng.*, **126**(5), 420-428. [https://doi.org/10.1061/\(ASCE\)1090-0241\(2000\)126:5\(420\)](https://doi.org/10.1061/(ASCE)1090-0241(2000)126:5(420)).
- Bartholomew, P. and Morris, A.J. (1976), "A unified approach to fully-stressed design", *Eng. Opt.*, **2**(1), 3-15. <https://doi.org/10.1080/03052157608960592>.
- Boulanger, R.W., Curras, C.J., Kutter, B.L., Wilson, D.W. and Abghari, A. (1999), "Seismic soil-pile-structure interaction experiments and analyses", *J. Geotech. Geoenviron. Eng.*, **125**(9), 750-759. [https://doi.org/10.1061/\(ASCE\)1090-0241\(1999\)125:9\(750\)](https://doi.org/10.1061/(ASCE)1090-0241(1999)125:9(750)).
- Bowles, J.E. (1996), *Foundation Analysis and Design*, 5th edition, McGraw-Hill, New York, NY, USA.
- Briseghella, B., Fenu, L., Feng, Y., Lan, C., Mazzarolo, E. and Zordan, T. (2016), "Optimization Indexes to Identify the Optimal Design Solution", *J. Bridge Eng.*, **21**(3), [https://doi.org/10.1061/\(ASCE\)BE.1943-5592.0000838](https://doi.org/10.1061/(ASCE)BE.1943-5592.0000838).
- Briseghella, B. and Zordan T. (2007), "Integral abutment bridge concept applied to the rehabilitation of a simply supported concrete structure", *Struct. Concr.*, **8**(1), 25-33.
- Briseghella, B. and Zordan T. (2015), "An innovative steel-concrete joint for integral abutment bridges", *J. Traff. Transp. Eng. (English Ed.)*, **2**(4), 209-222. <https://doi.org/10.1016/j.jtte.2015.05.001>.
- Briseghella, B., Fenu, L., Feng, Y., Mazzarolo, E. and Zordan, T. (2013), "Topology optimization of bridges supported by a concrete shell", *Struct. Eng. Int.*, **23**(3), 285-294.
- Briseghella, B., Fenu, L., Lan, C., Mazzarolo, E. and Zordan, T. (2013), "Application of topological optimization to bridge design", *J. Bridge Eng.*, **18**(8), 790-800. [https://doi.org/10.1061/\(ASCE\)BE.1943-5592.0000416](https://doi.org/10.1061/(ASCE)BE.1943-5592.0000416).
- Broms, B.B. (1964), "Lateral resistance of piles in cohesion less soils", *ASCE, J. Soil Mech. and Found. Div.*, **90**(3), 123-158.
- Broms, B.B. (1964), "Lateral resistance of piles in cohesive soils", *ASCE, J. of the Soil Mech. and Found. Div.*, **90**(2), 27-64.
- Brown, D.A. and Shie, C.F. (1990), "Three dimensional finite element model of laterally loaded piles", *Comp. Geotech.*, **10**(1), 59-79. [https://doi.org/10.1016/0266-352X\(90\)90008-J](https://doi.org/10.1016/0266-352X(90)90008-J).
- Caner, A. and Zia, P. (1998), "Behavior and design of link slabs for jointless bridge decks", *PCI journal*, **43**, 68-81.
- Carbonari, S., Morici, M., Dezi, F., Leoni, G., Nuti, C., Silvestri, F., Tropeano, G. and Vanzi, I. (2012), "Seismic response of viaducts accounting for soil-structure interaction", *Proceedings of the 15th World Conference on Earthquake Engineering*, Lisbon, Portugal, September.
- Chik, K.H., Abbas, J.M. and Taha, M.R. (2008), "Single pile simulation and analysis subjected to lateral load", *Electronic J. of Geotech. Eng.*, **13**.
- David, T.K. and Forth, J.P. (2011), "Modelling of soil structure interaction of integral abutment bridges", *J. Civil. Eng. Struct. Construct. Architect. Eng.*, **5**(6), 645-650.
- Davissou, M.T. (1970), "Lateral Load Capacity of Piles", *49th Annual Meeting of the Highway Research Board*, Washington, D.C., U.S.A., January. 104-112.
- Elsgolts, L.E. (1980), *Differential Equations and the Calculus of Variations, (English Edition)*, MIR Publishers, Moscow, USSR.
- Fenu, L. (2005), "On the characteristics of optimum beams with optimum length surrounded by a Winkler's medium", *Struct. Mult. Opt.*, **30**(3), 243-250. <https://doi.org/10.1007/s00158-004-0387-y>.
- Fenu, L. and Madama G. (2006), "Pali multiton caricati lateralmente e con spostamento minimo", *Proceedings of the 16th CTE Conference*, Parma, Italy, November.
- Fenu, L. and Serra, M. (1995), "Optimum design of beams surrounded by a Winkler's medium", *Struct. Opt.*, **9**(2), 132-135. <https://doi.org/10.1007/BF01758831>.
- Fenu, L., Briseghella, B. and Marano G.C. (2018), "Optimum shape and length of laterally loaded piles", *Struct. Eng. Mech.*, **68**(1), 121-130. <https://doi.org/10.12989/sem.2018.68.1.121>.
- Fiore, A., Marano, G.C., Greco, R. and Mastromarino, E. (2016), "Structural optimization of hollow-section steel trusses by

- differential evolution algorithm”, *J. Steel Struct.*, **16**(2), 411-423. <https://doi.org/10.1007/s13296-016-6013-1>.
- Gandomi, A.H. and Alavi, A.H. (2012), “A new multi-gene genetic programming approach to non-linear system modelling. Part II: Geotechnical and earthquake engineering problems”, *Neural Comput. Applic.*, **21**, 189-201. <https://doi.org/10.1007/s00521-011-0735-y>.
- Greco, R., Lucchini, A. and Marano, G.C. (2015), “Robust design of tuned mass dampers installed on multi-degree-of-freedom structures subjected to seismic action”, *Eng. Opt.*, **47**(8), 1009-1030. <https://doi.org/10.1080/0305215X.2014.941288>.
- Greco, R. and Marano, G.C. (2015), “Identification of parameters of Maxwell and Kelvin-Voigt generalized models for fluid viscous dampers”, *JVC/J. Vib. Control*, **21**(2), 260-274. <https://doi.org/10.1177/1077546313487937>.
- Greco, R., Marano, G.C. and Fiore, A. (2016), “Performance–cost optimization of Tuned Mass Damper under low-moderate seismic actions”, *Struct. Design Tall Special Build.*, **25**(18), 1103-1122. <https://doi.org/10.1002/ital.1300>.
- Haftka, R.T. and Gürdal, Z. (1993), *Elements of Structural Optimization*, Kluwer Academic Publishers, Dordrecht, Boston, London.
- Han, J. and Frost, J.D. (2000), “Load-deflection response of transversely isotropic piles under lateral loads”, *Int. J. for Num. and Anal. Meth. in Geomech.*, **24**(5), 509-529.
- Imancli, G., Kahyaoglu, M.R., Ozden, G., and Kayalar, A.S. (2009), “Performance functions for laterally loaded single concrete piles in homogeneous clays”, *Struct. Eng. Mech.*, **33**(4), 529-537. <http://doi.org/10.12989/sem.2009.33.4.529>.
- Juinarongrit, T. and Ashford, S.A. (2004), “Lateral load behaviour of cast-in-drilled-hole piles in weakly cemented sand”, *Transp. Res. Record. J. Transp. Res. Board*, **1868**, 190-198. <https://doi.org/10.3141/1868-20>.
- Kavitha, P.E., Beena, K.S. and Narayanan, K.P. (2016), “A review on soil–structure interaction analysis of laterally loaded piles”, *Innov. Infrastruct. Solut.* **1**(14). <https://doi.org/10.1007/s41062-016-0015-x>.
- Kim, W. and Laman, J.A. (2013), “Integral abutment bridge behavior under uncertain thermal and time-dependent load”, *Struct. Eng. Mech.*, **46**(1), 53-73. <https://doi.org/10.12989/sem.2013.46.1.053>.
- Kim, W., Laman, J.A. and Park, J.Y. (2014), “Reliability-based design of prestressed concrete girders in integral Abutment Bridges for thermal effects”, *Struct. Eng. Mech.*, **50**(3), 305-322. <https://doi.org/10.12989/sem.2014.50.3.305>.
- Kim, Y. and Jeong, S. (2011), “Analysis of soil resistance on laterally loaded piles based on 3d soil-pile interaction”, *Comp. Geotech.*, **2**, 248-257. <https://doi.org/10.1016/j.compgeo.2010.12.001>.
- Kok, S.T. and Huat B.B.K. (2008) “Numerical modelling of laterally loaded piles”, *American J. Appl. Sc.*, **5**(10), 1403-1408.
- Krishnamoorthy, A. and Sharma, K.J. (2008), “Analysis of single and group of piles subjected to lateral load using finite element method”, *Proceedings of the 12th International Conference of International Association for Computer Methods and Advances in Geomechanics (IACMAG)*, Goa, India, October. 3111-3116.
- Lan, C., Briseghella, B., Fenu, L., Xue, J. and Zordan, T. (2017), “The optimal shapes of piles in integral abutment bridges”, *J. Traff. Transp. Eng. (English. Ed.)*, **4**(6), 576-593. <https://doi.org/10.1016/j.jtte.2017.11.001>.
- Lavorato, D., Nuti, C., Santini, S., Briseghella, B. and Xue, J. (2015), “A repair and retrofitting intervention to improve plastic dissipation and shear strength of Chinese RC bridges”, *IABSE Conference, Geneva 2015: Structural Engineering: Providing Solutions to Global Challenges*, Geneva, Switzerland, September. 1762-1767.
- Marano, G.C. and Greco, R. (2011), “Optimization criteria for tuned mass dampers for structural vibration control under stochastic excitation”, *JVC/J. Vibration and Control*, **17**(5), 679-688.
- Marano, G.C., Greco, R., Quaranta, G., Fiore, A., Avakian, J. and Cascella, D. (2013), “Parametric identification of nonlinear devices for seismic protection using soft computing techniques”, *Adv. Mat. Res.*, **639-640**(1) 118-129. <https://doi.org/10.4028/www.scientific.net/AMR.639-640.118>.
- Marano, G.C., Trentadue, F. and Petrone, F. (2014), “Optimal arch shape solution under static vertical loads”, *Acta Mechanica*, **225**(3), 679-686. <https://doi.org/10.1007/s00707-013-0985-0>.
- Marano, G.C., Trentadue, F. and Greco, R. (2006), “Optimum design criteria for elastic structures subject to random dynamic loads”, *Eng. Optimization*, **38**(7), 853-871. <https://doi.org/10.1080/03052150600913028>.
- Marano, G.C., Trentadue, F. and Greco, R. (2007), “Stochastic optimum design criterion of added viscous dampers for buildings seismic protection”, *Struct. Eng. Mech.*, **25**(1), 21-37. <https://doi.org/10.12989/sem.2007.25.1.021>.
- McGann, C.R. and Arduino, P. (2011), Laterally-Loaded Pile Foundation; OpenSeesWiki. http://opensees.berkeley.edu/wiki/index.php/Laterally-Loaded_Pile_Foundation.
- McGann, C.R., Arduino, P. and Mackenzie-Helnwein, P. (2011), “Applicability of conventional p-y relations to the analysis of piles in laterally spreading soil”, *J. Geotech. Geoenviron. Eng.*, **137**(6), 557-567. [https://doi.org/10.1061/\(ASCE\)GT.1943-5606.0000468](https://doi.org/10.1061/(ASCE)GT.1943-5606.0000468).
- Myskis, A.D. (1979), *Advanced Mathematics for Engineers, (English Edition)*, MIR Publishers, Moscow, USSR.
- Nakhaee, M. and Johari, A. (2013), “Genetic based modelling of undrained lateral load capacity of piles in cohesion soils”, *Global J. Sci. Eng. Technology*, **5**, 123-133.
- Ng, K.W., Garder J. and Sriharan, S. (2015), “Investigation of ultra high performance concrete piles for integral abutment bridges”, *Eng. Str.*, **105**, 220-230. <https://doi.org/10.1016/j.engstruct.2015.10.009>.
- Palmer, L.A. and Thompson, J.B. (1948), “The earth pressure and deflection along the embedded lengths of piles subjected to lateral thrusts”, *Proceedings of the 2nd International Conference on Soil Mechanics and Foundation Engineering*, Rotterdam, The Netherlands. June.
- Patnaik, S.N. and Hopkins, D.A. (1998), “Optimality of a fully stressed design”, *Comp. Methods Appl. Mech. Eng.*, **165**(1-4), 215-221.
- Phanikanth, V.S., Choudhury, D. and Rami Reddy, G. (2010), “Response of single pile under lateral loads in cohesion less soils”, *Electronic J. Geotech. Eng.*, **15**.
- Poulos, H.G. and Davis, E.H. (1980), *Pile Foundation Analysis and Design*, John Wiley and Sons, Inc., New York, NY, USA.
- Quaranta, G., Marano, G.C., Greco, R. and Monti, G. (2014), “Parametric identification of seismic isolators using differential evolution and particle swarm optimization”, *Appl. Soft Comput. J.*, **22**, 458-464. <https://doi.org/10.1016/j.asoc.2014.04.039>.
- Reese, L.C. and Desai, C.S. (1977) “Laterally loaded piles”, *Numerical Methods in Geotechnical Engineering*, McGraw-Hill Book Company, New York, USA. 297-325.
- Wakai, A., Gose, S. and Ugai, K. (1999), “3D Elasto-plastic finite element analyses of pile foundations subjected to lateral loading”, *Soils and Foundations*, **39**(1), 97-111.
- Winkler, E. (1867), *Die Lehre von der Elastizität und Festigkeit*. Verlag Dominicus, Prague, Czech Republic.
- Xu, Z., Chen, B., Zhuang, Y., Tabatabai, H. and Huang, F. (2017), “Rehabilitation and retrofitting of a multispan simply-supported adjacent box girder bridge into a jointless and continuous structure”, *J. Performance Construct. Facilities*, **32**(1), [https://doi.org/10.1061/\(ASCE\)CF.1943-5509.0001107](https://doi.org/10.1061/(ASCE)CF.1943-5509.0001107).
- Yang, Z. and Jeremic, B. (2002), “Numerical analysis of pile behaviour under lateral loads in layered elastic-plastic soils”, *J.*

- Numer. Analyt. Methods Geo. Mech.*, **26**(14), 1-31.
<https://doi.org/10.1002/nag.250>.
- Zordan, T. and Briseghella, B. (2007), "Attainment of an integral abutment bridge through the refurbishment of a simply supported structure", *Struct. Eng. Int.*, **17**(3), 228-234.
<https://doi.org/10.2749/101686607781645824>.
- Zordan, T., Briseghella, B. and Lan, C. (2011), "Parametric and pushover analyses on integral abutment bridge", *Eng. Struct.*, **33**(2), 502-515. <https://doi.org/10.1016/j.engstruct.2010.11.009>.
- Zordan, T., Briseghella, B. and Mazzarolo, E. (2010), "Bridge structural optimization through step-by-step evolutionary process", *Struct. Eng. Int.*, **20**(1), 72-78.
<https://doi.org/10.2749/101686610791555586>.
- Zordan, T., Briseghella, B. and Lan C. (2011), "Analytical formulation for limit length of integral abutment bridges", *Struct. Eng. Int.*, **21**(3), 304-310.

CC